Acetylcholine Receptor Channels Activated by a Single Agonist Molecule

Archana Jha and Anthony Auerbach*
Department of Physiology and Biophysics, State University of New York, Buffalo, New York

ABSTRACT The neuromuscular acetylcholine receptor (AChR) is an allosteric protein that alternatively adopts inactive versus active conformations (**R** ↔ **R***). The **R*** shape has a higher agonist affinity and ionic conductance than **R**. To understand how agonists trigger this gating isomerization, we examined single-channel currents from adult mouse muscle AChRs that isomerize normally without agonists but have only a single site able to use agonist binding energy to motivate gating. We estimated the monoliganded gating equilibrium constant E_1 and the energy change associated with the **R** versus **R*** change in affinity for agonists. AChRs with only one operational binding site gave rise to a single population of currents, indicating that the two transmitter binding sites have approximately the same affinity for the transmitter ACh. The results indicated that $E_1 \approx 4.3 \times 10^{-3}$ with ACh, and $\approx 1.7 \times 10^{-4}$ with the partial-agonist choline. From these values and the diliganded gating equilibrium constants, we estimate that the unliganded AChR gating constant is $E_0 \approx 6.5 \times 10^{-7}$. Gating changes the stability of the ligand-protein complex by ~5.2 kcal/mol for ACh and ~3.3 kcal/mol for choline.

INTRODUCTION

Nicotinic acetylcholine receptors (AChRs) are ligand-gated ion channels that trigger fast transmission at the vertebrate neuromuscular synapse (1–3). Each AChR has five subunits ($\alpha_2\beta\delta\varepsilon$, in adult muscle) and two transmitter binding sites (one in the extracellular domain of each α subunit near the adjacent δ or ε subunit). Acetylcholine (ACh) released from the nerve terminal occupies these sites to initiate a global, gating conformational change in the protein that leads to the depolarization of the muscle membrane.

AChRs are able to isomerize between nonconducting and conducting shapes (**R** ↔ **R***) both with and without agonists present at the binding sites, by approximately the same sequence of intramolecular events (4,5). In addition to having a higher ionic conductance, **R*** also has a higher affinity for agonists, and it is this difference in ligand-binding energy that causes the gating equilibrium constant to increase substantially when the binding sites are occupied by, for example, the transmitter ACh. To understand how exogenous molecules motivate gating, it is of value to quantify the **R** versus **R*** difference in binding energy experienced by agonists at each site. Without an external energy source, the ratio of gating equilibrium constants with one versus no bound agonist molecule (E_1/E_0) is equal to the ratio of agonist equilibrium dissociation constants of that binding site in **R** versus **R*** (K_d/J_d) (1). Here, we estimate the E_1/E_0 ratio, and hence the change in binding energy, by studying AChRs that have only one site able to use ligands to set in motion the gating conformational change.

It is still not known with certainty whether the two AChR transmitter binding sites have the same affinity for ACh. The **R** affinities of these two sites for the antagonist curare (6–8) and some protein toxins (9–11) differ substantially. The location of the binding sites near subunit interfaces provides a structural rationale for such different affinities for these relatively large ligands. Also, on theoretical grounds it has been proposed that synaptic performance is better optimized by having distinct binding-site affinities for the transmitter (12). However, the experimental evidence regarding the affinities for ACh at the two binding sites is equivocal. Some single-channel kinetic studies have reported distinct ACh affinities at the two sites (13–15), whereas others have found no such difference (16–18). It has been suggested that the omission of a short-lived nonconducting state (whose lifetime is independent of the agonist concentration (19)) from the single-channel modeling studies leads to the incorrect designation of one binding site as having a very low affinity for the agonist (18). One of our objectives in this study was to resolve the issue of transmitter binding-site equality more definitively by making direct, single-channel measurements of the functional properties of AChRs with only a single site capable of using agonist-binding energy for gating.

These measurements offered a new method for estimating E_0 and the energy made available for gating by the change in the affinity of the protein for the agonist. By measuring E_1 experimentally (for each site), and with prior knowledge of the diliganded equilibrium constant E_2, we were able to calculate the affinity ratios for the two binding sites, and hence E_0, for adult mouse neuromuscular AChRs. The results show that the two binding sites have approximately the same affinity for ACh in both **R** and **R***, and that **R** → **R*** gating decreases the equilibrium dissociation constant for ACh or choline by a factor of ~6600 or 270 (−5.2 or −3.3 kcal/mol). The magnitudes of these energies provide a foundation for understanding how ligands coax proteins to change shape.

Submitted October 29, 2009, and accepted for publication January 14, 2010.

*Correspondence: auerbach@buffalo.edu

Editor: Richard W. Aldrich.

0006-3495/10/05/1840/7 $2.00

doi: 10.1016/j.bpj.2010.01.025

MATERIALS AND METHODS

Mutations of mouse AChR subunit cDNAs were made by using the QuickChange site-directed mutagenesis kit (Stratagene, La Jolla, CA), and verified by nucleotide sequencing. Human embryonic kidney fibroblast cells (HEK 293) were transiently transfected using calcium phosphate precipitation method. HEK cells were treated with 3.5–5.5 μg DNA per 35-mm culture dish in the ratio of 2:1:1:1 (α:β:δ:ε) for ~16 h. Most electrophysiological recordings were made ~24 h later. For hybrid experiments, HEK cells were transfected in a cDNA ratio of 1:1:1:1:1. Recordings were performed in a cell-attached patch configuration at 23°C. Agonist was dissolved in the pipette solution (Dulbecco's phosphate-buffered saline) containing (in mM) 137 NaCl, 0.9 $CaCl_2$, 2.7 KCl, 1.5 KH_2PO_4, 0.5 $MgCl_2$, and 8.1 Na_2HPO_4 (pH 7.3). The bath solution was identical to the pipette solution. The pipettes were made from borosilicate capillaries and coated with Sylgard (Dow Corning, Midland, MI). The average pipette resistance was ~10 MΩ. The pipette potential was held at +70 mV, which corresponds to a membrane potential of ~−100 mV. Single-channel currents were recorded using a PC-505 amplifier (Warner Instruments, Hamden, CT). For most experiments, the currents were low-pass-filtered at 20 kHz and digitized at a sampling frequency of 50 kHz using a SCB-68 acquisition board (National Instruments, Austin, TX). For the cross-concentration experiments, the currents were sampled at 100 kHz. All recording and analyses were done with the use of QUB software (http://www.qub.buffalo.edu).

For rate constant analysis, clusters of individual-channel activity were selected so that the flanking, nonconducting intervals were ≥50 ms. Clusters were idealized into noise-free intervals after they were filtered digitally (12 kHz) by using the segmental *k*-means algorithm (20) with a two-state, C(losed) ↔ O(pen) model (starting rate = 10 s^{-1}). The opening and closing rate constants were estimated from the idealized interval durations by using a maximum-interval likelihood algorithm (21) after imposing a dead time of 50 μs. Usually, the rate constants were estimated by using a two-state model because the log likelihood of the fit did not increase after additional C or O states were added. In some patches, a second nonconducting state was connected to the open state to accommodate a relatively rare and short-lived state associated with desensitization (19).

The apparent values of the monoliganded forward (f_1) and backward (b_1) isomerization rate constants underestimate the true values (Table 1). First, even at high agonist concentrations, the (single) wild-type (wt) binding site is not completely saturated, and the apparent intracluster, closed-channel inverse lifetime is less than f_1 by a factor $F = ([A]/K_d)/(1+([A]/K_d))$, where A is the agonist and K_d is the **R** equilibrium dissociation constant (~140 μM for ACh, ~4 mM for choline in wt AChRs). We calculate that $F \approx 0.78$ at 500 μM ACh and 0.83 at 20 mM choline. Second, the apparent b_1 underestimates the true backward isomerization rate constant because unresolved, fast channel-block by the agonist prolongs the apparent **R*** lifetime. For this correction, we used the ratio of the current amplitude at 10 μM ACh, where there is essentially no channel block (i_0; ~7 pA) to the current amplitude at 500 μM ACh (or 20 mM choline), where such a block pertains (i_B). We made the first-order approximation that the blocking agonist molecule only dissociates from the **R*** conformation of the pore, in which case the block prolongs openings in proportion to the i_0/i_B ratio: $b_1^{corrected} = b_1^{apparent}(i_0/i_B)$ (22).

TABLE 1 Gating rate and equilibrium constants for un- and monoliganded AChRs

[Agonist] mM		Construct		n	f, s^{-1}	b, s^{-1}	E_0 ($\times 10^3$)	E_1 ($\times 10^3$)
		αW149	background					
0	ACh	W (wt)	DYS	-	187*	3994*	47.0*	
0	ACh	M	DYS	3	148(13)	4988(278)	30.0	
0	ACh	L	DYS	3	30(9)	8732(542)	3.4	
0.5	ACh	M+W	wt	4	17(03)	5037(633)		3.7
0.5	ACh	M+W	αS269I	3	415(49)	1320(104)		3.3
0.5	ACh	L+W	αS269I	3	329(19)	2375(158)		5.2
0.5	ACh	M+W	αD97F	4	375(30)	2673(300)		4.6
20	Cho	M+W	αP272A	5	69(18)	643(133)		0.17

DYS is the AChR construct α(D97A+Y127F+S269I), which increases E_0 by a factor of ~10^6; *, from Purohit and Auerbach (5); n, number of patches; uncorrected rate constants: f, forward **R** → **R*** (mean ± SE for n patches); b, backward **R** ← **R***. E_0, unliganded equilibrium constant; E_1, monoliganded equilibrium constant. E_1 was calculated after correction for subsaturation of the binding site, channel block by the agonist, and the change in E_0 caused by the background mutations (see Materials and Methods). The average value for all constructs with ACh is $E_1 = 4.3 \pm 0.4 \times 10^{-3}$ (mean ± SE). The diliganded equilibrium constants (E_2) for ACh and choline are 28 (31) and 4.6×10^{-2} (28). The ratio E_2/E_1 (which is equal to the K_d/J_d affinity ratio) for these agonists is 6600 and 270. E_1 divided by this ratio is E_0, 6.6×10^{-7} and 6.3×10^{-7}, respectively.

In some experiments, monoliganded clusters of openings were measured in AChRs with a gain-of-function background mutation (αS269I, αD97F, or αP272A). We corrected for the background perturbation by assuming that the fold changes in f_1 and b_1 caused by the mutations were the same as previously measured for diliganded receptors; that is, we assumed that the background mutation increased E_0 by 91-fold (αS269I (23)), 31-fold (αD97F (24)), or 237-fold (αP272A (25)). The fact that these corrections all led to similar E_0 estimates supports the hypothesis that these mutations only perturb E_0 and do not significantly alter the isomerization conformational pathway(s) or the agonist affinity ratio (5) (Table 1).

We also made a small correction for the effects of the αW149M and αW149L binding-site mutations on E_0. These double mutations (one at each of the two binding sites) decreased unliganded gating (E_0) by 1.5-fold and 13.8-fold, respectively. As a first approximation, we assumed that this effect was equally divided between the two binding sites, and therefore multiplied the apparent E_1 values (after the above corrections for saturation, block, and background) by the square root of the corresponding fold change in E_0.

AChRs that have αW149M or αW149L mutations at both binding sites can be activated by very high ACh concentrations, which indicates that this ligand is not acting as an inverse agonist at the mutated binding site (the **R/R*** affinity ratio is >1; P. Purohit and A. Auerbach, unpublished observations). Preliminary results for double-mutant αW149M AChRs show $K_d > 10$ mM and $E_2 \approx 3 \times 10^{-3}$. We estimate that at 500 μM ACh, >95% of the hybrid AChRs are monoliganded. These constructs have low activity in 500 μM ACh (Fig. 1 *B*) because they have both a low affinity and a low affinity ratio for ACh.

The association (k_+) and dissociation (k_-) rate constants for ACh binding were estimated from intracluster interval durations obtained at different ACh concentrations. The interval durations at all concentrations were fitted together by using a kinetic model (C ↔ AC ↔ AO, where A is ACh) that had four rate constants: k_+, k_-, f_1 (AC → AO) and b_1 (AC ← AO). With the $\alpha 149_{(W+L)}$+αS269I construct, in the fit all four rate constants were free parameters. With the $\alpha 149_{(W+M)}$+αS269I construct, f_1 was fixed at 520 s^{-1}.

RESULTS

Our experimental approach was to express AChRs that isomerize normally (i.e., have an E_0 value similar to that of wt AChRs) but are able to utilize agonist-binding energy at only one of the two transmitter binding sites. We would not have been able to achieve that goal by using site-specific antagonists, because the affinity ratios for such ligands are unknown.

Each α subunit has a conserved binding-site Trp residue (αW149) that is an important determinant of ACh affinity (26,27). Fig. 1 shows the effects of mutating this residue, in both the absence and presence of ACh, on two different background constructs. Without any exogenous agonists,

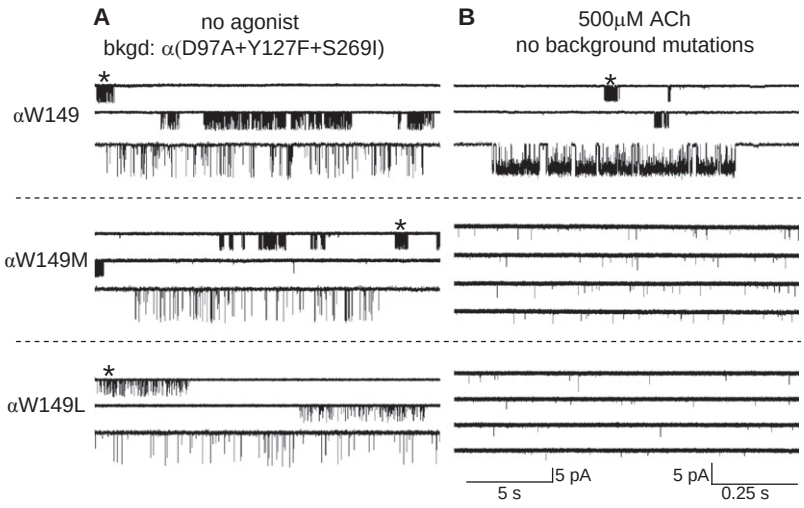

FIGURE 1 αW149 mutations allow spontaneous gating but eliminate gating by 500 μM ACh. (*A*) Spontaneous activity (in the absence of agonists) of AChRs with three gain-of-function background mutations that greatly increase the unliganded gating equilibrium constant, E_0 (αD97A+αY127F+αS269I). Top: Single-channel currents from the background construct alone. Each cluster represents the **R**↔**R*** activity of a single, unliganded AChR (conducting is down); long gaps between clusters are periods when all AChRs in the patch are desensitized; bottom trace is expanded view of marked currents. Middle and bottom: Spontaneous currents after adding a binding-site (αW149) mutation (Met or Leu, respectively). These mutations have only a modest effect on E_0 (Table 1). (*B*) Activity of AChRs exposed to 500 μM ACh (wt background, which shows very little spontaneous gating). Top: The open probability within clusters is high because the AChRs without any αW149 mutations are able to bind and use energy from ACh at both transmitter binding sites. Middle and bottom: The binding-site (αW149) mutations reduce the frequency of openings because they are unable to bind ACh or use energy from the agonist affinity change to trigger gating. Left and right calibrations are for low- and high-resolution views throughout.

individual AChRs with multiple background mutations (which together increase E_0 by a factor of ~10^6) open spontaneously in clusters, each of which reflects the activity of an individual AChR (5). Fig. 1 *A* and Table 1 show that mutating αW149 (in both α subunits) to Met or Leu has only a modest effect on the apparent unliganded equilibrium constant. This result indicates that the αW149M and αW149L constructs are able to isomerize spontaneously between **R** and **R*** conformations much like wt AChRs.

Fig. 1 *B* shows that on a wt background (which has a very low probability of opening spontaneously), either of these mutations greatly reduces the ability of AChRs to be activated by a 500 μM ACh. Because the E_0 values of the mutants are only slightly different from that of the wt, the failure of αW149M and αW149L AChRs to generate clusters in the presence of ACh indicates that at this ACh concentration the mutant binding sites are unable to utilize ligand-binding energy to significantly increase the isomerization equilibrium constant (see Materials and Methods).

The key experiment was to coexpress both αW149M and αW149 (wt) α subunits along with wt β, δ, and ε subunits. This protocol is expected to lead to four different AChR populations. Some of the expressed AChRs should have W-W at position α149 at the two binding sites, and some should have M-M. There should also be two hybrid populations, with W-M or M-W at the two binding sites. Because the double-mutant αW149M mutation has only a small effect on E_0 (a ~1.5-fold reduction), and because this mutation essentially eliminates activation by 500 μM ACh, both hybrid constructs should be able to isomerize normally but with only one binding site capable of using energy from the transmitter molecule. Thus, the single-channel currents from the hybrid clusters activated by 500 μM ACh should exclusively reflect the activity of AChRs activated by just one agonist molecule.

Fig. 2 *A* shows clusters of openings from a αW149M hybrid experiment, using an otherwise wt background. At 500 μM ACh, high open-probability clusters generated by doubly liganded wt (W-W) AChRs are apparent, as are occasional, isolated openings arising from the inefficient, double-mutant (M-M) constructs. In addition, a new population of clusters was observed, which we interpret as arising from the activity of the monoliganded, hybrid constructs W-M and M-W. After several corrections to the rate constants (see Materials and Methods), we estimate from this construct that for wt AChRs, $E_1^{ACh} = 3.7 \times 10^{-3}$ (Table 1).

With the wt background, the hybrid clusters were of long duration and had a low open probability and were therefore difficult to isolate and quantify. We therefore added a gain-of-function background mutation to both the αW149 and αW149-mutant α subunits. αS269I (in the transmembrane, M2 helix) increases E_0 by 91-fold, does not influence agonist binding and has equal and independent effects on the gating equilibrium constant in the two α subunits (23,28,29). Fig. 2 *B* shows example clusters from experiments using this background mutation. Again, clusters from diliganded, W-W AChRs and isolated openings from broken, M-M AChRs were apparent, along with clusters of openings arising from hybrid AChRs. In all patches, only a single hybrid population was apparent (Fig. 2 *C*), with both the conducting and nonconducting intervals within the clusters having single-exponential distributions (Fig. 2 *D*). After correction, from this construct we estimate that in wt AChRs, $E_1^{ACh} = 3.3 \times 10^{-3}$ (Table 1).

We also examined monoliganded clusters from αW149M hybrids expressed on a different background mutation: αD97F

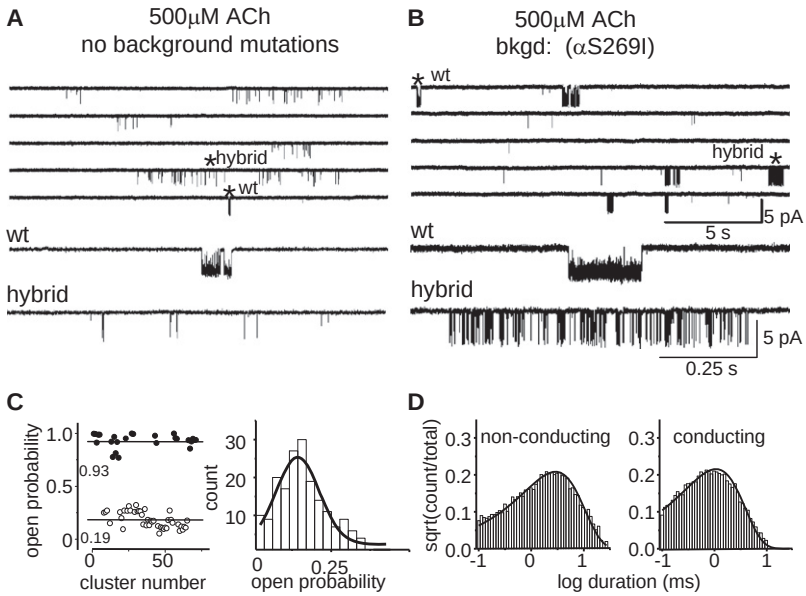

FIGURE 2 Gating activity of monoliganded (hybrid) AChRs activated by ACh. (*A*) Activity of hybrid AChRs (wt background) exposed to 500 μM ACh. The AChRs had a combination of αW149 and αW149M residues at the two transmitter binding sites. The bottom two traces are marked openings at an expanded scale. Diliganded AChRs with two αW149 residues (wt; W-W) can use ACh binding energy to open efficiently and therefore produce high open-probability clusters. Monoliganded (hybrid) AChRs with one αW149 and one αW149M (hybrid; W-M and M-W) can use ACh binding energy at only one transmitter binding site and therefore produce lower open-probability clusters. (*B*) Activity of fully liganded, hybrid AChRs with the gain-of-function background mutation αS269I (Table 1). The AChRs had a combination of αW149 and αW149M residues at the two transmitter binding sites. In the low-resolution view, the sporadic, isolated openings reflect M-M AChRs that cannot utilize ACh binding energy. Marked clusters from wt and hybrid AChRs are shown below. (*C*) Cluster population analysis (αS269I background). Left: Both diliganded (W-W) high open-probability clusters (0.93; *solid circles*) and monoliganded (W-M and M-W) low open-probability clusters (0.19; *open circles*) are apparent in a single patch. Right: The monoliganded population, fitted by a single Gaussian. There is only one monoliganded population. (*D*) The conducting and nonconducting intervals within the monoliganded clusters are each fitted by a single exponential.

(see Fig. S1 in the Supporting Material). The results were similar to those obtained with the wt and αS269I backgrounds (Table 1). Fig. S1 also shows the results of experiments using the αW149L mutation and the αS269I background. Again, in all patches only a single population of hybrid clusters was apparent. The E_1 estimates for all of the AChR constructs were within a factor of 1.6. This supports the hypothesis that the background mutations act independently and only by changing E_0. From all hybrid experiments combined, we estimate that for wt AChRs, $E_1^{ACh} = 4.3 \times 10^{-3}$ (Table 1).

To test whether the single population of clusters reflected AChRs having either one functional α_ε or one functional α_δ site, we coexpressed δ subunits having the mutation δW57A (Fig. S2). This mutation, which is on the minus side of the α_δ transmitter binding site, reduces the **R** affinity of only that site by ~28-fold (30), so at 500 μM ACh this site would not be saturated by the agonist (14% occupancy versus

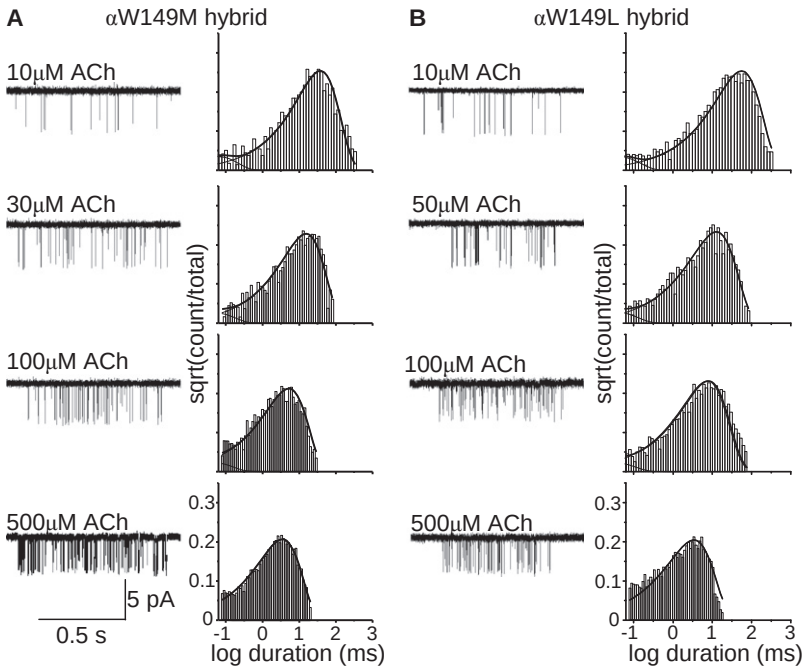

FIGURE 3 ACh binding parameters for monoliganded AChRs. (*A*) Results for αW149M hybrid AChRs (*background*, αS269I) activated by various [ACh]. For each panel: (*left*) example hybrid clusters; (*right*) intracluster, nonconducting interval histograms and probability density functions (*solid line*) computed from global model-fitting across concentrations (see Materials and Methods). The estimated rate constants ($\pm$SD) were as follows: association 153 $\pm$ 53 $\mu M^{-1}s^{-1}$ and dissociation 19,969 $\pm$ 9410 s^{-1} (equilibrium dissociation constant: 131 μM; number of intervals: 5198). The published estimates for the association and dissociation rate constants for wt AChRs, assuming equal binding sites, are 167 μM^{-1} s^{-1} and 24,745 s^{-1}, respectively (18). (*B*) Results for αW149L hybrid AChRs (*background*, αS269I) activated by various [ACh]. The estimated rate constants were as follows: association, 126 $\pm$ 32 $\mu M^{-1}s^{-1}$; dissociation, 18,099 $\pm$ 4609 s^{-1} (equilibrium dissociation constant: 144 μM; number of intervals: 10,218).

78% occupancy for the wt site; see Materials and Methods). Two populations of monoliganded clusters were apparent in this experiment: one having approximately the same open probability as without the δW57A mutation, and one with a lower open probability. We conclude that the single population of hybrid clusters observed without the δW57A mutation arises from monoliganded AChRs, with both single-α_ε and -α_δ sites contributing. This experiment also shows that the hybrid AChRs contained both δ and ε subunits.

We next determined for hybrid clusters the ACh association (k_+) and dissociation (k_-) rate constants and their ratio, the equilibrium dissociation constant ($K_d = k_-/k_+$). Fig. 3, *A* and *B*, show the results of fitting intracluster current interval durations from W/M and W/L hybrid populations obtained over a range of ACh concentrations. The estimated rate constants were as follows: $k_+ = 153\ \mu M^{-1}s^{-1}$, $k_- = 19{,}969\ s^{-1}$, and $K_d = 131\ \mu M$ (M hybrid); and $k_+ = 126\ \mu M^{-1}s^{-1}$, $k_- = 18{,}099\ s^{-1}$, and $K_d = 144\ \mu M$ (L hybrid). These rate and equilibrium constants are similar to each other and essentially the same as those estimated from fitting wt AChRs assuming equal and independent binding sites: $k_+ = 167\ \mu M^{-1}\ s^{-1}$, $k_- = 24{,}745\ s^{-1}$, and $K_d = 148\ \mu M$ (16,18).

We repeated the hybrid experiments using choline as the agonist. Fig. 4 shows monoliganded clusters from αW149M hybrid AChRs expressed on the background P272A (a mutation that increases E_0 by 237-fold (25)). With this partial agonist, only one hybrid population was apparent. We estimate that for wt AChRs, $E_1^{choline} = 1.7 \times 10^{-4}$ (Table 1).

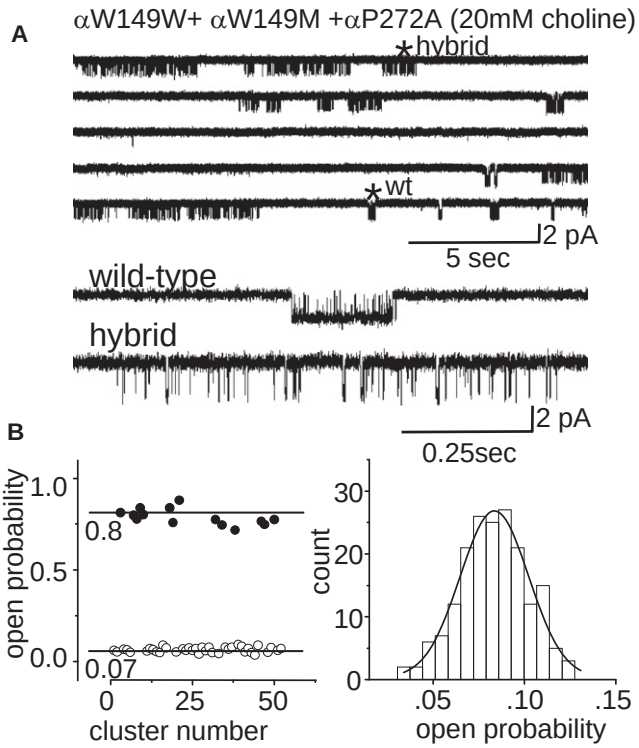

FIGURE 4 Gating activity of monoliganded (hybrid) AChRs activated by choline. (*A*) Activity of fully liganded and hybrid AChRs with the gain-of-function background mutation αP272A and activated by choline (Table 1). The AChRs had a combination of αW149 and αW149M residues at the two transmitter binding sites. Marked clusters from wt and hybrid AChRs are shown below. (*B*) Cluster population analysis. Left: Both diliganded (W-W) high open-probability clusters (0.80; *solid circles*) and monoliganded (W-M and M-W) low open-probability clusters (0.07; *open circles*) are apparent in a single patch. Right: The monoliganded population, fitted by a single Gaussian. There is only one population of monoliganded AChRs.

DISCUSSION

In the hybrid experiments, we observed only a single population of clusters arising from monoliganded AChRs (Figs. 2 *C* and 4 *B*). The ACh association and dissociation rate constants for this population are the same as for wt AChRs assuming two equal and independent transmitter binding sites (Fig. 3). These results indicate that the two adult mouse neuromuscular AChR transmitter binding sites are approximately the same with regard to ACh binding. The transmitter binding sites are located near subunit interfaces, but there is no indication that this structural fact has a significant effect on the binding function of AChRs at the mouse neuromuscular synapse. We estimate that for each transmitter binding site, the **R** equilibrium dissociation constant for ACh is ~140 μM, which is the ratio of the dissociation rate constant (~20,000 s^{-1}) and the association rate constant (~$1.4 \times 10^8\ M^{-1}s^{-1}$).

To estimate the monoliganded gating equilibrium constant (E_1), we made several corrections to the apparent rate constants (see Materials and Methods, and Table 1). With these adjustments we estimate that the wt, monoliganded equilibrium gating equilibrium constants (−100 mV membrane potential, 23°C) are $E_1^{ACh} \approx 4.3 \times 10^{-3}$ and $E_1^{choline} \approx 1.7 \times 10^{-4}$.

Estimates of the diliganded equilibrium constants (E_2) for these two agonists for adult mouse AChRs are available: $E_2^{ACh} = 28$ (31) and $E_2^{choline} = 4.6 \times 10^{-2}$ (28). Because the energy available from agonist binding (the K_d/J_d affinity ratio) for the two sites is identical, $E_2/E_1 = E_1/E_0$. Hence, $E_0 = E_1^2/E_2$. Of significance, the E_0 values calculated by using this relationship were essentially the same for ACh and choline. The average for all backgrounds and agonists was $E_0 \approx 6.5 \times 10^{-7}$ (Table 1).

E_0 was previously estimated by a completely different method that used exclusively unliganded AChRs (5). By measuring spontaneous gating in constructs that had various combinations of background mutations that each increased E_2 to known extents, and by assuming that the mutations were independent and had no effect on the affinity ratio, we estimated an average value: $E_0 \approx 1.2 \times 10^{-7}$. Another E_0 estimate can be gained from these same data by extrapolating to the condition of no change in E_2, in which case $E_0 \approx 7.7 \times 10^{-7}$. The E_0 estimate obtained from hybrid analyses falls within these limits, but it, too, is imprecise. The experimental E_1^{ACh} values vary by 1.6-fold (Table 1),

and published estimates of E_2^{ACh} vary to a similar degree. We think that $E_0 \approx 6.5 \times 10^{-7}$ is currently the best estimate, but more experiments will likely increase the precision to which we know the magnitude of this fundamental gating equilibrium constant.

It is extremely valuable to have an accurate estimate of E_0 because we can use it to calculate all of the rate and equilibrium constants for AChR activation (Fig. S3). At each binding site, we estimate that the **R**/**R*** affinity ratio ($=E_2/E_1$) is ~6600 for ACh and ~270 for choline. These values translate to a per-site difference in agonist-binding energy (**R*** versus **R**) of ~−5.2 kcal/mol for ACh and ~−3.3 kcal/mol for choline. For ACh, the equilibrium dissociation constant from **R** ≈ 140 μM, so that from **R*** ≈ 20 nM. The ACh dissociation rate constant from **R*** is ~12 s^{-1} (32), so the corresponding association rate constant is ~5×10^8 $M^{-1}s^{-1}$. Gating hardly alters the rate constant at which ACh enters the transmitter binding sites.

It will be worthwhile to explore the extents to which binding and gating parameters are the same or different for other receptor channels and for different agonists. It will also be interesting to learn the atomic forces that generate the net binding energies for different ligands (e.g., the ~1.9 kcal/mol difference between ACh and choline) or different AChRs with binding-site mutations. Finally, we would like to know whether the conformational pathway of the **R** ↔ **R*** isomerization is the same for AChRs asymmetrically activated by only a single agonist as it appears to be for un- and diliganded AChRs.

SUPPORTING MATERIAL

Three figures are available at http://www.biophysj.org/biophysj/supplemental/S0006-3495(10)00158-X.

We thank Dr. P. Purohit for sharing his knowledge about the αW149 mutants, and M. Merritt, M. Shero, and M. Teeling for technical assistance.

This work was supported by the National Institutes of Health (NS-23513 and NS-064969).

REFERENCES

1. Auerbach, A. 2010. The gating isomerization of neuromuscular acetylcholine receptors. *J. Physiol.* 588:573–586.
2. Edelstein, S. J., and J. P. Changeux. 1998. Allosteric transitions of the acetylcholine receptor. *Adv. Protein Chem.* 51:121–184.
3. Sine, S. M., and A. G. Engel. 2006. Recent advances in Cys-loop receptor structure and function. *Nature*. 440:448–455.
4. Jackson, M. B. 1984. Spontaneous openings of the acetylcholine receptor channel. *Proc. Natl. Acad. Sci. USA*. 81:3901–3904.
5. Purohit, P., and A. Auerbach. 2009. Unliganded gating of acetylcholine receptor channels. *Proc. Natl. Acad. Sci. USA*. 106:115–120.
6. Neubig, R. R., and J. B. Cohen. 1979. Equilibrium binding of [3H]tubocurarine and [3H]acetylcholine by Torpedo postsynaptic membranes: stoichiometry and ligand interactions. *Biochemistry*. 18:5464–5475.
7. Pedersen, S. E., and J. B. Cohen. 1990. d-Tubocurarine binding sites are located at α-γ and α-δ subunit interfaces of the nicotinic acetylcholine receptor. *Proc. Natl. Acad. Sci. USA*. 87:2785–2789.
8. Sine, S. M. 1993. Molecular dissection of subunit interfaces in the acetylcholine receptor: identification of residues that determine curare selectivity. *Proc. Natl. Acad. Sci. USA*. 90:9436–9440.
9. Molles, B. E., I. Tsigelny, …, P. Taylor. 2002. Residues in the epsilon subunit of the nicotinic acetylcholine receptor interact to confer selectivity of waglerin-1 for the α-epsilon subunit interface site. *Biochemistry*. 41:7895–7906.
10. Osaka, H., S. Malany, …, P. Taylor. 1999. Subunit interface selectivity of the α-neurotoxins for the nicotinic acetylcholine receptor. *J. Biol. Chem.* 274:9581–9586.
11. Sine, S. M., H. J. Kreienkamp, …, P. Taylor. 1995. Molecular dissection of subunit interfaces in the acetylcholine receptor: identification of determinants of α-conotoxin M1 selectivity. *Neuron*. 15: 205–211.
12. Jackson, M. B. 1989. Perfection of a synaptic receptor: kinetics and energetics of the acetylcholine receptor. *Proc. Natl. Acad. Sci. USA*. 86:2199–2203.
13. Jackson, M. B. 1988. Dependence of acetylcholine receptor channel kinetics on agonist concentration in cultured mouse muscle fibres. *J. Physiol.* 397:555–583.
14. Sine, S. M., T. Claudio, and F. J. Sigworth. 1990. Activation of Torpedo acetylcholine receptors expressed in mouse fibroblasts. Single channel current kinetics reveal distinct agonist binding affinities. *J. Gen. Physiol.* 96:395–437.
15. Sine, S. M., K. Ohno, …, A. G. Engel. 1995. Mutation of the acetylcholine receptor α subunit causes a slow-channel myasthenic syndrome by enhancing agonist binding affinity. *Neuron*. 15:229–239.
16. Akk, G., and A. Auerbach. 1996. Inorganic, monovalent cations compete with agonists for the transmitter binding site of nicotinic acetylcholine receptors. *Biophys. J.* 70:2652–2658.
17. Colquhoun, D., and D. C. Ogden. 1988. Activation of ion channels in the frog end-plate by high concentrations of acetylcholine. *J. Physiol.* 395:131–159.
18. Salamone, F. N., M. Zhou, and A. Auerbach. 1999. A re-examination of adult mouse nicotinic acetylcholine receptor channel activation kinetics. *J. Physiol.* 516:315–330.
19. Elenes, S., and A. Auerbach. 2002. Desensitization of diliganded mouse muscle nicotinic acetylcholine receptor channels. *J. Physiol.* 541: 367–383.
20. Qin, F. 2004. Restoration of single-channel currents using the segmental *k*-means method based on hidden Markov modeling. *Biophys. J.* 86:1488–1501.
21. Qin, F., A. Auerbach, and F. Sachs. 1997. Maximum likelihood estimation of aggregated Markov processes. *Proc Biol Sci.* 264:375–383.
22. Purohit, Y., and C. Grosman. 2006. Block of muscle nicotinic receptors by choline suggests that the activation and desensitization gates act as distinct molecular entities. *J. Gen. Physiol.* 127:703–717.
23. Grosman, C., F. N. Salamone, …, A. Auerbach. 2000. The extracellular linker of muscle acetylcholine receptor channels is a gating control element. *J. Gen. Physiol.* 116:327–340.
24. Chakrapani, S., T. D. Bailey, and A. Auerbach. 2003. The role of loop 5 in acetylcholine receptor channel gating. *J. Gen. Physiol.* 122:521–539.
25. Jha, A., D. J. Cadugan, …, A. Auerbach. 2007. Acetylcholine receptor gating at extracellular transmembrane domain interface: the cys-loop and M2-M3 linker. *J. Gen. Physiol.* 130:547–558.
26. Akk, G. 2001. Aromatics at the murine nicotinic receptor agonist binding site: mutational analysis of the αY93 and αW149 residues. *J. Physiol.* 535:729–740.
27. Zhong, W., J. P. Gallivan, …, D. A. Dougherty. 1998. From ab initio quantum mechanics to molecular neurobiology: a cation-π binding site in the nicotinic receptor. *Proc. Natl. Acad. Sci. USA*. 95:12088–12093.
28. Mitra, A., G. D. Cymes, and A. Auerbach. 2005. Dynamics of the acetylcholine receptor pore at the gating transition state. *Proc. Natl. Acad. Sci. USA*. 102:15069–15074.

29. Purohit, Y., and C. Grosman. 2006. Estimating binding affinities of the nicotinic receptor for low-efficacy ligands using mixtures of agonists and two-dimensional concentration-response relationships. *J. Gen. Physiol.* 127:719–735.

30. Bafna, P. A., A. Jha, and A. Auerbach. 2009. Aromatic residues εTrp-55 and δTrp-57 and the activation of acetylcholine receptor channels. *J. Biol. Chem.* 284:8582–8588.

31. Chakrapani, S., and A. Auerbach. 2005. A speed limit for conformational change of an allosteric membrane protein. *Proc. Natl. Acad. Sci. USA.* 102:87–92.

32. Grosman, C., and A. Auerbach. 2001. The dissociation of acetylcholine from open nicotinic receptor channels. *Proc. Natl. Acad. Sci. USA.* 98:14102–14107.